agriculture

MDPI

Article

Dielectric Properties of Hydrothermally Modified Potato, Corn, and Rice Starch

Chong You Beh [1], Ee Meng Cheng [1,2,*], Nashrul Fazli Mohd Nasir [1,3], Mohd Shukry Abdul Majid [4], Shing Fhan Khor [5], Mohd Ridzuan Mohd Jamir [4], Emma Ziezie Mohd Tarmizi [6] and Kim Yee Lee [7]

1 Faculty of Electronic Engineering Technology, Universiti Malaysia Perlis (UniMAP), Arau 02600, Malaysia; chongyou@studentmail.unimap.edu.my (C.Y.B.); nashrul@unimap.edu.my (N.F.M.N.)
2 Advanced Communication Engineering, Centre of Excellence (CoE), Universiti Malaysia Perlis (UniMAP), Kangar 01000, Malaysia
3 Sports Engineering Research Centre (SERC), Universiti Malaysia Perlis (UniMAP), Arau 02600, Malaysia
4 Faculty of Mechanical Engineering Technology, Universiti Malaysia Perlis (UniMAP), Arau 02600, Malaysia; shukry@unimap.edu.my (M.S.A.M.); ridzuanjamir@unimap.edu.my (M.R.M.J.)
5 Faculty of Electrical Engineering Technology, Universiti Malaysia Perlis (UniMAP), Arau 02600, Malaysia; sfkhor@unimap.edu.my
6 Centre of Foundation Studies for Agricultural Science, Universiti Putra Malaysia, Serdang 43400, Malaysia; emma@upm.edu.my
7 Lee Kong Chian Faculty of Engineering & Science, Sungai Long Campus, Tunku Abdul Rahman University, Jalan Sungai Long, Kajang, Cheras, Sungai Long City 43000, Malaysia; kylee@utar.edu.my
* Correspondence: emcheng@unimap.edu.my

Abstract: The effect of starch granule sizes, shapes, composition, and frequency on the dielectric properties (dielectric constant, loss factor, and conductivity) of native and hydrothermally modified starches (potato, corn, and rice starch) are investigated in this work. Dielectric properties are determined from 5 Hz to 5 GHz. The modified starches exhibit lower dielectric properties than the native starches from 5 Hz to 5 GHz due to the disruption of the native polysaccharide's molecular arrangement. The modified potato starch shows the highest loss factor (208.12 at 50 Hz and 19.95 at 500 Hz) and stable conductivity (~5.33×10^{-7} S/m at 50 Hz and 500 Hz) due to the larger continuous network structure after hydrothermal modification. The rice starch shows the largest difference in dielectric constant (47.30%) and loss factor (71.42%) between the modified form and native form in the frequency range of 5 MHz–5 GHz. This is due to the restriction of dipole motions in the closely packed structure after hydrothermal modification. The findings indicate that the quality of starch modification can be characterized by dielectric properties for assisting starch-based plastic production's design.

Keywords: polymeric carbohydrate; relative complex permittivity; conductivity; gelatinization; recrystallization

Citation: Beh, C.Y.; Cheng, E.M.; Mohd Nasir, N.F.; Abdul Majid, M.S.; Khor, S.F.; Mohd Jamir, M.R.; Mohd Tarmizi, E.Z.; Lee, K.Y. Dielectric Properties of Hydrothermally Modified Potato, Corn, and Rice Starch. *Agriculture* **2022**, *12*, 783. https://doi.org/10.3390/agriculture12060783

Academic Editor: Hongbin Pu

Received: 21 April 2022
Accepted: 27 May 2022
Published: 29 May 2022

1. Introduction

Starch is a macromolecule that is abundant in nature, inexpensive, renewable, biodegradable, and easy to process. It is widely used in the food, pharmaceutical, biomedical, and chemical industries nowadays [1–3]. Starch is subjected to numerous physical/chemical treatments to modify its structure for the functional properties (physicochemical, optical, electrical, and dielectric properties) required for specific technological applications [3,4]. There is growing interest in developing biodegradable plastics derived from natural resources to mitigate the environmental pollution caused by plastic waste. Potato, corn, and rice starches are potential sources of biodegradable plastics. These starches are environmentally friendly. Potato, corn, and paddy (rice) are widely cultivated throughout the world and will eventually replace petroleum-based plastics [5–7]. Starch granules are typically composed of alternatively arranged semicrystalline and amorphous regions.

These regions are composed of polysaccharide macromolecules (linear-chain amylose and branched-chain amylopectin) [8,9]. The physicochemical, functional, and structural properties of starch vary greatly with the amylose/amylopectin ratio [9,10]. Starch also contains trace constituents (lipid, protein, ash, and phosphorus) that affect starch properties [11,12]. Water is commonly used to plasticize native starch granules due to its effectiveness. The structure of the polysaccharide macromolecules in plasticized starch granules is modified physically [13,14].

In hydrothermal treatment (thermal action in the presence of water), water diffuses into the starch granule regions and triggers a series of starch granular structure disruptions [2,15]. The starch granules subsequently swell due to amorphous regions that are destabilized by water absorption. The water-saturated amorphous regions expand and transmit disruptive stress to the semicrystalline regions of the starch granule [2,14]. The semicrystalline regions in starch granules start to melt and transform into an amorphous liquid state, subject to hydrothermal effects (mechanical shear stress and heat) [10,16,17]. This eventually interrupts granular organization and causes the collapse of the granule structure. Subsequently, the amylose molecules leach from the granules as the molecular mobility increases [6,13,14]. During cooling, the disaggregated polysaccharide macromolecules reassociate and gradually realign into a structure that differs from those in native granules [8,18]. Amylose and amylopectin molecules start to incorporate with other polysaccharide macromolecules and recrystallize into double helices through intermolecular interactions [13,18]. The infinite aggregation of the double helices generates a higher-order three-dimensional crystalline network structure and crystallinity through the formation of hydrogen bonds during water expulsion [17–19]. Native starch can be recrystallized by hydrothermal modification, which disrupts native starch structures and facilitates interaction between polysaccharide chains within the amorphous and crystalline domains.

Starch is susceptible to a variety of property-altering treatments, which results in uncertainty of the modified starch's characteristics for further material design. The potential changes in the starch granule structures after complete recrystallization are crucial for investigating the complexity of starch-based plastic production processes that expedite the improvement of starch-based plastic production. Dielectric spectroscopy provides interesting insights into the grain boundary, grain structure, charge storage capabilities, and electrical transport properties of the material [9,20,21]. Dielectric spectroscopy is widely used in investigating the polarization of a material in response to an oscillation of an applied electric field. It describes the dielectric properties of a material. Dielectric properties are a function of operating frequency, chemical composition, microstructure, and other factors [9,21,22]. Changes in the physicochemical characteristics of modified starch alter the electric dipole orientation and space charge mobility when interacting with microwave or radio frequency fields, thereby affecting the dielectric properties of the material system. These dielectric properties are the rapid and nondestructive preliminary parameters for evaluating the starch phase transition qualities (granular variation, molecular weight distribution, structural defect, and material interaction) during starch-based plastic development [2,22,23]. Reorientation of the dipoles of the main/segmental polymer chains and charge migration within the material under an applied electric field are the primary mechanisms of electromagnetic radiation absorption in starch-based plastics [4,20,22]. The starch-based material absorbs electromagnetic radiation due to the molecular polarity and granular structure [20,21,24]. Several past studies were conducted regarding the influence of temperature, water content, and gelatinization on the dielectric properties of various native/gelatinized starches [1,4,15]. However, the dielectric response of the native starches has not been adequately investigated over a wide frequency range. Meanwhile, there is no information available on the study of the dielectric properties of the recrystallized starches after physical modification.

In this study, the physically modified starches were fabricated using hydrothermal treatment (gelatinization and recrystallization) and water (which acts as a plasticizer of native starch). Frequency-dependent dielectric properties (dielectric constant, loss factor,

and conductivity) were measured from 5 Hz to 5 GHz using the impedance analyzer and vector network analyzer. The study aims to investigate and compare the dielectric properties of starches from different sources, i.e., potato, corn, and rice in the native form and modified form (after hydrothermal modification). This study hypothesized that structural changes and polysaccharide molecular interactions of modified starches could be evaluated through electrical responses that are influenced by starch granule sizes, shapes, composition, and frequency. Herein, we identify possible factors that cause the spectrum between native and modified forms of starch to vary in terms of the effect of starch granule sizes, shapes, composition, and frequency. This research may provide new perspectives for rapidly characterizing changes in starch molecular and granular structure. This study attempts to gain a better understanding of the quality of starch modification (material interactions) after being subjected to gelatinization and recrystallization via dielectric characterization techniques. It has paramount importance in starch-based plastic production's design and material characterization.

2. Materials and Methods

2.1. Sample Preparations

Commercial native potato starch (native-Ps), corn starch (native-Cs), and rice starch (native-Rs) were used. The composition and morphological properties of the starches are shown in Table 1 [6,8,12,25]. The starch suspension was prepared by dispersing native starch in distilled water and stirring for 15 min at 25 °C. The ratio of native starch to distilled water was 1:3. Next, the starch suspension was heat pre-treated in the temperature range of 55–65 °C for about 1 h. The pre-heated starch suspension was continuously stirred at 300 rpm and heated at 95 °C for 15–25 min in a water bath. Subsequently, the gelatinized samples were rapidly cooled to room temperature and then kept at 4 °C for 12 h. Then, the modified starch was prepared by dehydrating the sample at a temperature range of 75–85 °C for 24 h. The dried samples were ground into a fine powder using a mortar and pestle and compacted into disk-form pellets (20 mm diameter, 3 mm thickness) using a uniaxial hydraulic press. Lastly, the samples were kept in a vacuum desiccator before characterization. The physically modified potato starch, corn starch, and rice starch are denoted as modified-Ps, modified-Cs, and modified-Rs, respectively, in this work.

Table 1. Composition and morphological properties of native starches.

	Potato	**Corn**	**Rice**
Granule shape	Lenticular	Spherical/polyhedral	Polyhedral
Size (μm)	5–100	2–30	3–8
Average diameter (μm)	36	15	5
Amylose (%)	18	28	35
Amylopectin (%)	82	72	65
Lipid (%)	0.1	0.6–0.8	0.6–1.4
Protein (%)	0.1	0.4	0.1–0.5
Ash (%)	0.2	0.1	0.1
Phosphorus (%)	0.09	0.01	0.07

2.2. Sample Characterizations

The dielectric properties are denoted by the complex permittivity, ε*. This describes the interaction of a material with the applied electric field, as expressed in Equation (1):

$$\varepsilon^* = \varepsilon' - j\varepsilon'' \quad (1)$$

where ε' is the dielectric constant and ε'' is the loss factor. The dielectric constant (ε') and the loss factor (ε''), which correspond to the real and imaginary parts of the relative complex permittivity (ε*), are the dielectric properties of greatest interest in material characterizations. The relative complex permittivity is the dielectric property that describes the behavior of a material when it is placed in an electromagnetic field [9,15]. The dielectric

constant indicates the ability of a material to store electrical energy and polarize when subjected to an electric field, whereas the loss factor indicates the ability of the material to dissipate energy in the form of heat in response to an applied electric field [9,26]. According to the Debye principle, dielectric properties are related to conductivity, which provides significant indices that can be used to determine the electrical response of a material to an applied electric field [27,28]. The HIOKI IM3570 impedance analyzer was used to conduct impedance measurements in the parallel capacitance and conductance mode (C_p-G) from 5 Hz to 5 MHz. The parallel capacitance (C_p) and conductance (G) were measured by placing the studied sample under test in between two copper electrodes that were connected to the impedance analyzer via the L2000 4-terminals probe. The impedance measurement was conducted at room temperature with the excitation of oscillated voltage in 1.0 V. ε', ε'' and conductivity (σ), are expressed in Equations (2)–(4):

$$\varepsilon' = \frac{C_P d}{A\varepsilon_0} \tag{2}$$

$$\varepsilon'' = \frac{Gd}{\varepsilon_0 A\omega} \tag{3}$$

$$\sigma = \frac{Gd}{A} \tag{4}$$

where A is the base area of the studied sample, d is the thickness of the sample, ε_0 is the free space permittivity (8.85×10^{-12} F/m), and $\omega(=2\pi f)$ is the angular frequency [3,29].

For the frequency range of 5 MHz to 5 GHz, the dielectric properties of the samples were measured with an open-ended coaxial-line probe kit in conjunction with the Agilent Technologies E5071C ENA series vector network analyzer. The vector network analyzer and probe kit need to be calibrated using the Short-Open-Load calibration standard, which consists of a short-circuit block, air, and distilled water at 25 °C. The sample pellet makes contact with the aperture of the probe. The measurements are taken at room temperature. The complex reflection coefficient (S_{11}^*) of the sample is determined using Agilent Technologies 85070E dielectric probe kit software to compute the dielectric constant (ε'), loss factor (ε''), and conductivity (σ). In a capacitive approach, the S_{11}^* can be expressed as Equation (5):

$$S_{11}^* = |S_{11}|e^{j\varphi} = \frac{1 - j\omega Z_0(\varepsilon^* C_0 + C_f)}{1 + j\omega Z_0(\varepsilon^* C_0 + C_f)} \tag{5}$$

where $|S_{11}|$ and φ are the magnitude and phase of the complex reflection coefficient, respectively. In the meantime, the ε', ε'', and σ can be determined via Equations (6)–(8):

$$\varepsilon' = \frac{-2|S_{11}|\sin\varphi}{\omega C_0 Z_0\left(1 + 2|S_{11}|\cos\varphi + |S_{11}|^2\right)} - \frac{C_f}{C_0} \tag{6}$$

$$\varepsilon'' = \frac{1 - |S_{11}|^2}{\omega C_0 Z_0\left(1 + 2|S_{11}|\cos\varphi + |S_{11}|^2\right)} \tag{7}$$

$$\sigma = \omega\varepsilon_0\varepsilon'' \tag{8}$$

where C_0 is the free space capacitance, C_f is the fringe field capacitance, and Z_0 is the characteristic impedance of the coaxial line probe [28,30,31].

3. Results and Discussion

3.1. Dielectric Constant and Loss Factor over 5 Hz–5 MHz

The variation of ε' and ε'' of the native starches and modified starches over the frequency range of 5 Hz–5 MHz are shown in Figures 1 and 2, respectively. In Figures 1 and 2, ε' and ε'' of the native and modified form of starches decreased as the frequency increased. This might be mainly ascribed to the reduction in the Maxwell–Wagner–Sillars interfacial

polarization effect. In the low-frequency region, the space charges of the samples have sufficient time to realign with the oscillation of the applied electric field. The interfacial polarization effect is minimized as the frequency increases, because the space charges of the samples are unable to react rapidly in full polarization before the polarity of the oscillated electric field changes [21,23].

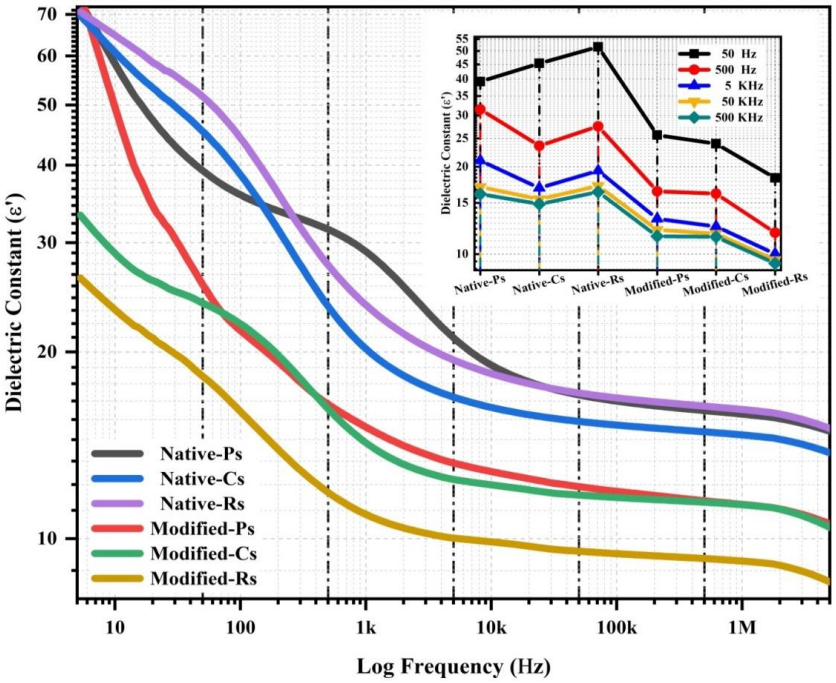

Figure 1. Frequency dependence of dielectric constant of native form and modified form of starches over the log frequency.

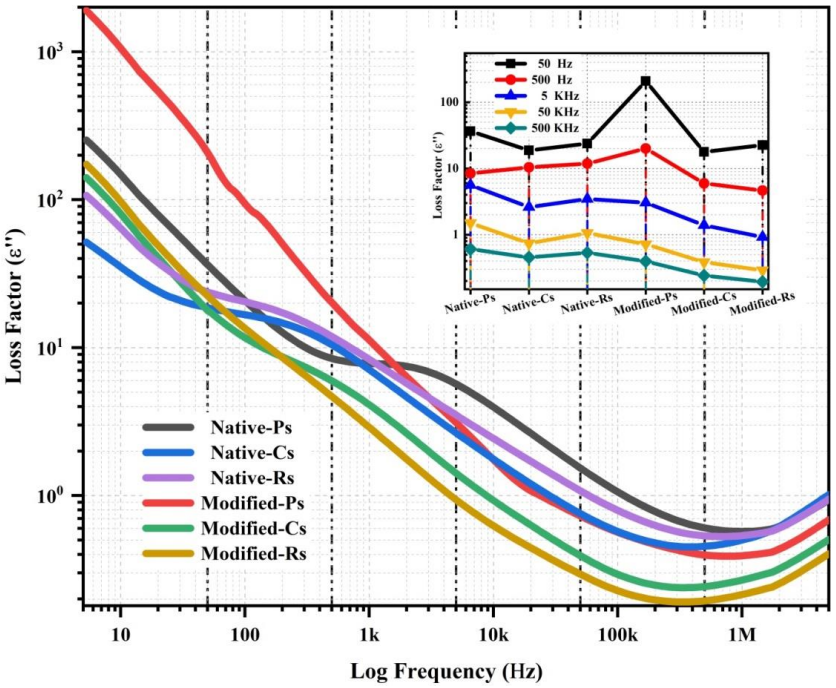

Figure 2. Frequency dependence of loss factor of native form and modified form of starches over the log frequency.

Native potato starch is found to have regular and lenticular shape granules (5–100 μm) with concentric striations. Native corn starch is presented in the homogenous spherical and polygonal granules (2–30 μm) with a distinct cavity in the center or 2–5 rays cleft. Native rice starch has irregular and polygonal granules (3–8 μm) with a simple or compound structure. This structure has about 2–150 polyhedral components [8,12,25,32]. A schematic diagram for the native starch granule structure is shown in Figure 3. At 50 Hz, the native-Rs exhibit the highest ε' of 51.62, followed by the native-Cs (45.36) and native-Ps (39.23), as shown in Figure 1. This might be due to the compound structure of the native rice starch granules and the sharp-edged polyhedrons that lead to a vast amount of insulating grain boundaries for the accumulation of the space charges, which results in the increment of the interfacial polarization [33,34]. On the other hand, the polygonal-shaped granules of the native corn and rice starch exhibit the angular sides that imply the ability of starch granules to form a close-packed structure (as shown in Figure 3). This is beneficial to the progress of the pile up and polarization of the space charges at the grain boundary [3,8,33].

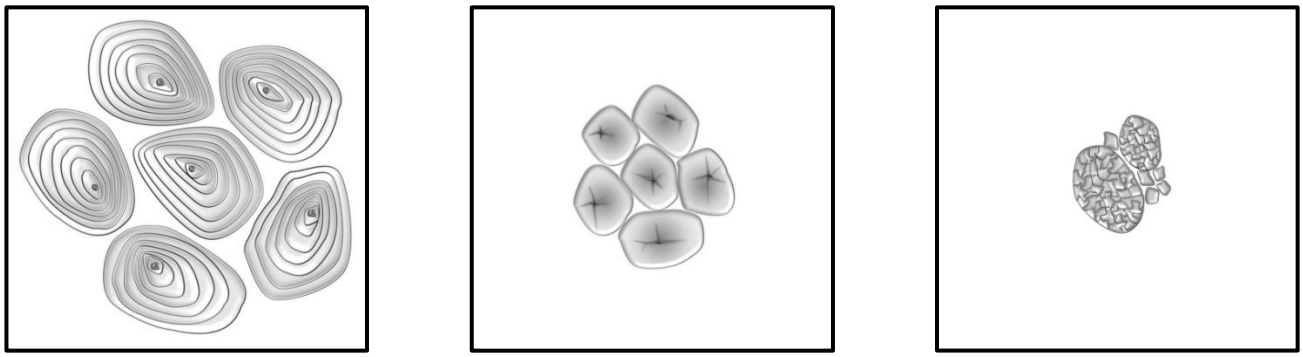

(**a**) (**b**) (c)

Figure 3. Native starch granule structure: (**a**) potato starch, (**b**) corn starch, and (**c**) rice starch.

However, the native-Ps show the highest ε' (31.48 at 500 Hz and 20.97 at 5 kHz) compared with the native-Rs (27.52 at 500 Hz and 19.37 at 5 kHz) and native-Cs (23.60 at 500 Hz and 16.88 at 5 kHz) at the frequency of 500 Hz and 5 kHz. Potato starch exhibited the highest average granule size (36 μm in diameter), followed by corn starch (15 μm in diameter). Meanwhile, rice starch shows the smallest average granule size (5 μm in diameter) [8,25]. The results show that the larger granule size of the native potato starch significantly induces space charge accumulations at the grain boundary to create a potential barrier for interfacial polarization [3,21,24]. It is also clearly indicated that the modified starches exhibit a lower ε' compared to the native starches. This might be attributed to the structural rupture of the starch granules when they are subjected to hydrothermal modification, and the defects of the grain boundaries reduce the capability of the accumulation of the space charges [21,22,33]. The modified-Rs show the lowest ε' compared with the native-Rs from 5 Hz–5 MHz. This is because the modified-Rs experience a drastic decrement, by roughly 112.77%. The ε' of the modified-Cs decreases by about 46.44% when compared with the native-Cs. Meanwhile, the ε' of the modified-Ps decreased by about 35.30% when compared with the native-Ps within 5 Hz–5 MHz. The ε' of the modified-Ps is higher than that of the modified-Rs from 5 Hz–5 MHz, as shown in Figure 1. This might be due to the hydrothermal modification that leads to the destruction of the native rice starch. The destruction is more significant than in the native potato and corn starch. The modified rice starch fails to maintain a native granular structure due to disruption of the starch granules. The modified corn starch and potato starch can mitigate further rupture to the native granular structure due to the stability of their native granular structures and higher amylopectin content (which is primarily responsible for the starch granule's structural rigidity) [8,11,35]. Thus, the interfacial polarizability of the modified rice starch is highly reduced, because it lacks grain boundaries for the

space charge polarization. In the high-frequency range, the ε' of all samples remains constant. This indicates that dipole polarization, instead of the interfacial polarization, plays a predominant role and starts to take effect [1,27].

In Figure 2, the native form of the starches shows the decrement order of the loss factor as native-Ps >native-Rs > native-Cs for the frequency at 50 Hz, 5 kHz, 50 kHz, and 500 kHz. This might be due to the concentric layer structures of the native potato starch (as shown in Figure 3a) that result in a higher energy dissipation of the space charge migration when it is subjected to the time-varying electric field. Meanwhile, the native rice starch granules in polyhedral compound structures (as shown in Figure 3c) dissipate more heat energy during interfacial polarization when compared with the simple polyhedral structures of the native corn starch granules (as shown in Figure 3b) [3,21,28]. In addition, the native-Ps show a lower ε'' (8.43) compared with the native-Cs (10.39) and native-Rs (11.81) at 500 Hz, as shown in Figure 2. This might be associated with the larger granular size of the native potato starch, which is independent of energy dissipation during the interfacial polarization at 500 Hz [9,21]. The ε'' of the modified-Cs and modified-Rs is generally lower than that of the native forms of the starches from 5 Hz–5 MHz, but not for the modified-Ps. It can be noticed that the ε'' of the modified-Ps (208.12 at 50 Hz and 19.95 at 500 Hz) is greater than that of the native-Ps (36.38 at 50 Hz and 8.43 at 500 Hz) at the frequency of 50 Hz and 500 Hz. Meanwhile, the modified-Ps exhibit a higher ε'', followed by the modified-Cs and modified-Rs, within the 5 Hz–5 MHz frequency range, as shown in Figure 2. Generally, the ε'' of the modified starches over frequency is expected to be lower than that of the native starches when the interfacial polarizability of the modified starches recedes. However, this might be attributed to the recrystallization of the native potato starch into a larger continuous network structure after the hydrothermal modification, which can enhance the energy dissipation during the interfacial polarization, especially in a low-frequency region [3,8,34].

3.2. Dielectric Constant and Loss Factor over 5 MHz–5 GHz

Figures 4 and 5 display the variation of the ε' and ε'' versus frequency (5 MHz–5 GHz) for the native and modified forms of the starches, respectively. In Figure 4, the ε' of the native and modified forms of the starches decreased steadily when the frequency was increased from 0.5 GHz to 5.0 GHz, and it decreased significantly at a lower frequency region, i.e., <0.5 GHz. At low frequencies, the permanent and induced dipoles can align synchronously with the oscillation of the electric field. As the frequency increases, the dipoles are unable to fully polarize with respect to the oscillating polarity of the applied field. A full polarization requires dipoles to react synchronously with the time-varying electric field [26,28]. Hence, the ε' spectra of the samples show a steep high gradient in the low-frequency region, whereas a lower gradient can be observed in the high-frequency region. As shown in Figure 4, the ε' of the native-Ps is the highest in the 5 MHz–5 GHz range. However, the ε' of the native-Rs (5.34) exhibits a higher value than the native-Cs (5.22) at 0.5 GHz. The dipole polarization plays a major role from 5 MHz to 5 GHz. The native rice starch has the highest amylose content, at 35%, as shown in Table 1. At lower frequencies, linear amylose molecules align more readily than large, branched amylopectin molecules to achieve full polarization when subjected to an oscillating electric field. Hence, the contribution of the amylose molecules becomes insignificant, whereas the effect of the amylopectin molecules becomes prominent in the dipole polarization when the frequency increases. The presence of the amylopectin molecules' side-chain branches might lead to a significant increment in the dipole's diffusion when it is subjected to the oscillated electric field [1,2,23,36]. Thus, the native potato starches (amylopectin content of 82%) are easier to conduct full dipole polarization when compared with the native corn starch (amylopectin content of 75%) and native rice starch (amylopectin content of 65%).

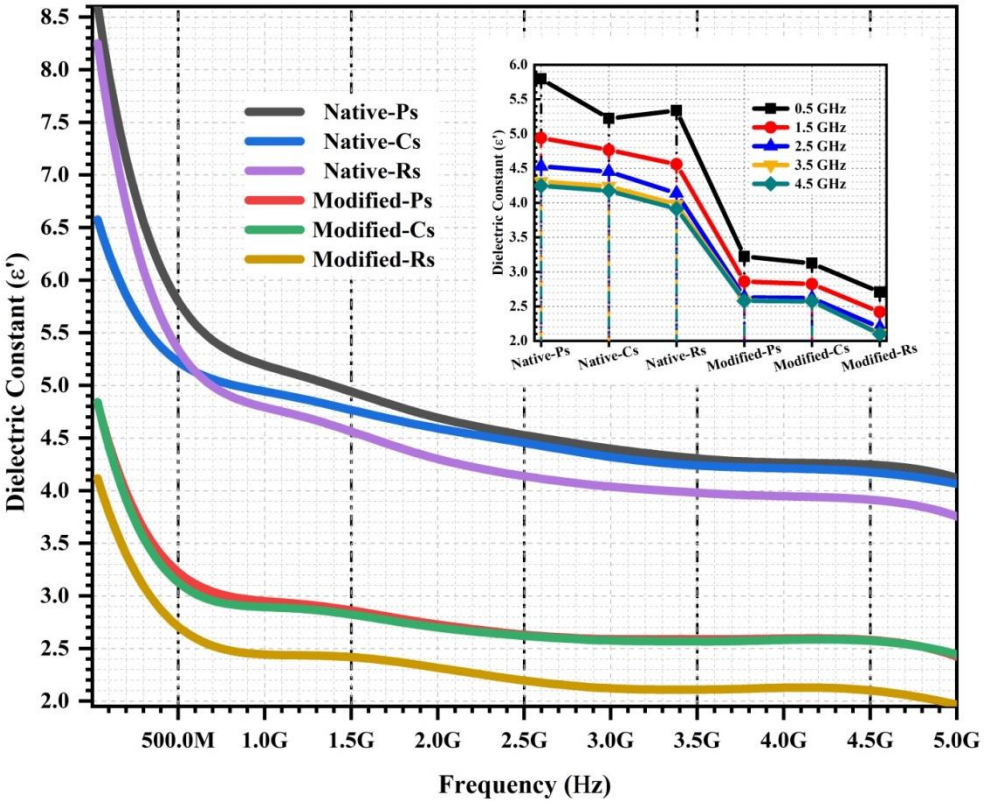

Figure 4. The variation in ε' of native and modified of starches over the frequency.

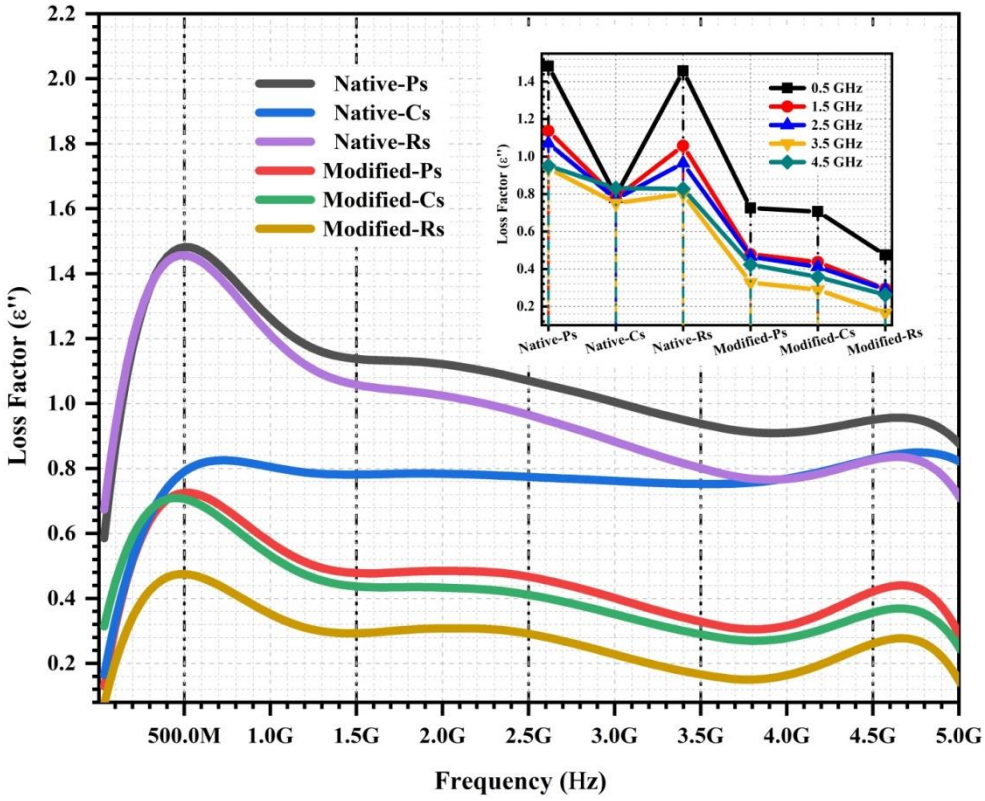

Figure 5. The variation in ε'' of native and modified starches over the frequency.

The ε' of the native starches is greater than that of the modified starches, as shown in Figure 4. The difference in ε' between the modified and native forms of rice starch

was the largest (47.30%) in the 5 Hz–5 MHz range. In the range of 5 MHz–5 GHz, the ε' of the modified-Ps is decreased by about 41.50% compared with the native-Ps, whereas the ε' of the modified-Cs is decreased by about 39.97% compared with the native-Cs. Meanwhile, the ε' of the modified-Rs is lower than that of the modified-Ps. The modified-Cs and modified-Ps have a similar ε'. The unrestricted rotational and vibrational motion of the dipoles (full polarization) results in a higher ε' of the native starches when exposed to an oscillating electric field. However, the modified starches exhibit a close-packed structure via recrystallization, using the leached polysaccharide molecules to link the starch granules to form a recrystallized continuous network structure that promotes restricted dipole movement, resulting in a lower ε'. Figure 6 depicts a schematic diagram of the recrystallized starch chain distribution. Native rice starch has a higher amylose content compared to the other native starches, which is associated with a higher tendency to recrystallize after hydrothermal modification. The significant decrement in the ε' of rice starch is attributed to the charge immobilization induced by the formation of abundant intermolecular hydrogen bonds in the modified rice starch after recrystallization [4,11,35]. In the frequency range of 5 MHz–5 GHz, the ε'' of native-Ps is higher than that of native-Rs and native-Cs, as shown in Figure 5. The native rice starch with lower amylopectin content is presumed to have a lower molecular weight than the native potato starch and native corn starch. The lower molecular weight of the native rice starch might be due to ineffective energy dissipation, resulting in the lowest ε'' [37,38]. However, the native-Cs have a lower ε'' than the native-Rs. When compared to native-Ps and native-Rs, the ε'' of the native-Cs appears frequency-independent from 1.5 GHz to 3.5 GHz. Meanwhile, the ε'' of the native-Cs seems frequency-independent from 1.5–3.5 GHz when compared with the native-Ps and native-Rs. This might be due to the lower degree of polymerization of the native corn starch's polysaccharide macromolecules (amylose and amylopectin) compared with the native rice starch. The native corn starch might be insensitive to the variation of frequency of the applied electric field, and it has a low energy dissipation [11,12,26].

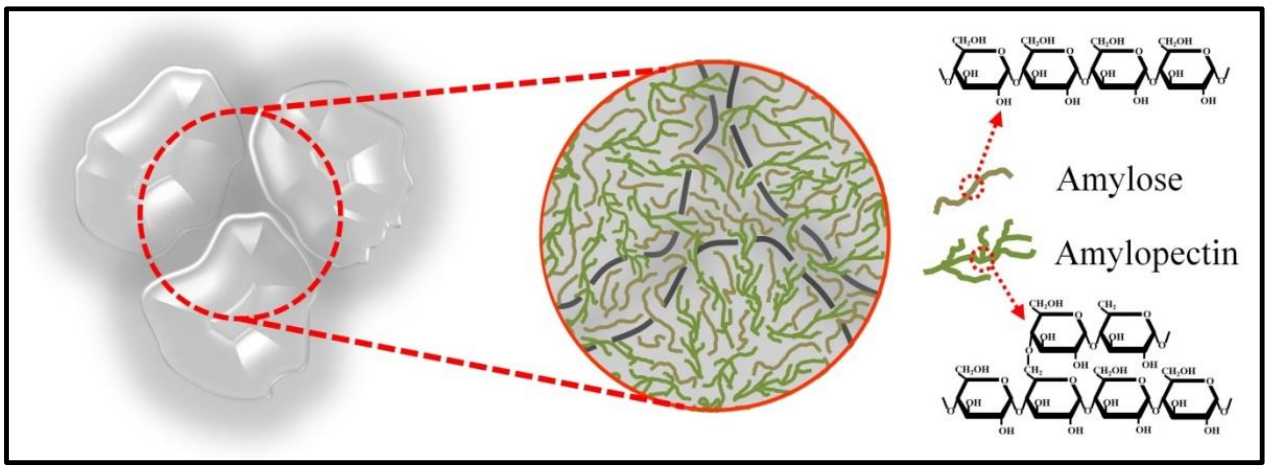

Figure 6. Schematic representation of the recrystallized starch chain distribution.

As seen in Figure 5, the ε'' of the native and modified forms of the starches exhibits two peaks, at 0.5 GHz and 4.5 GHz. It can be observed that ε' exhibits a major decline from 5 MHz-1 GHz and a minor decline from 4–5 GHz (Figure 4). The relaxation peak implies the rotations of the permanent dipoles that fail to react synchronously with the oscillation of the applied field as the frequency exceeds the relaxation frequency of the starches, resulting in a higher dissipation of energy and the presence of the maximum peak of ε''. This might be mainly due to the presence of the hydroxyl side groups (–OH) and hydroxymethyl side group (–CH_2OH) of the starches, which carry permanent dipole moments [2,9,22]. The loss factor reduction is relatively larger (71.42%) for the modified-Rs when compared with the other samples in the frequency range of 5 MHz–5 GHz. In the

range of 5 MHz–5 GHz, the ε'' of the modified-Ps decreases by about 57.18% compared with the native-Ps, whereas the ε'' of the modified-Cs decreases by about 44.06% compared with the native-Cs. The ε'' of the modified-Ps is higher than that of the other modified starches, as shown in Figure 5. The high amylose content leads to the recrystallization of the native rice starch into a closely packed structure with a high order after hydrothermal modification. The cancellation of dipole moments between the reordered hydroxyl side groups (–OH) and hydroxymethyl side group (–CH_2OH) of the recrystallized rice starches at each alternating carbon backbone is due to their directions, which oppose one another. Thus, the decrement in the ε'' can be attributed to the reduction in dipole moments in the amylose content of the modified starches [11,24,35].

3.3. Electrical Conductivity over 5 Hz–5 MHz and 5 MHz–5 GHz

Figures 7 and 8 show the frequency-dependent σ for all the samples from 5 Hz–5 MHz and 5 MHz–5 GHz. Figure 7 exhibits the average lower σ spectrum from 5 Hz–5 MHz than the σ spectrum from 5 MHz–5 GHz in Figure 8. The frequency-dependent properties of the σ are associated with the hopping of charge carriers from one localized state to another upper state in the conduction band. Charge carrier hopping can be accelerated by increasing the frequency of the applied electric field [27,28].

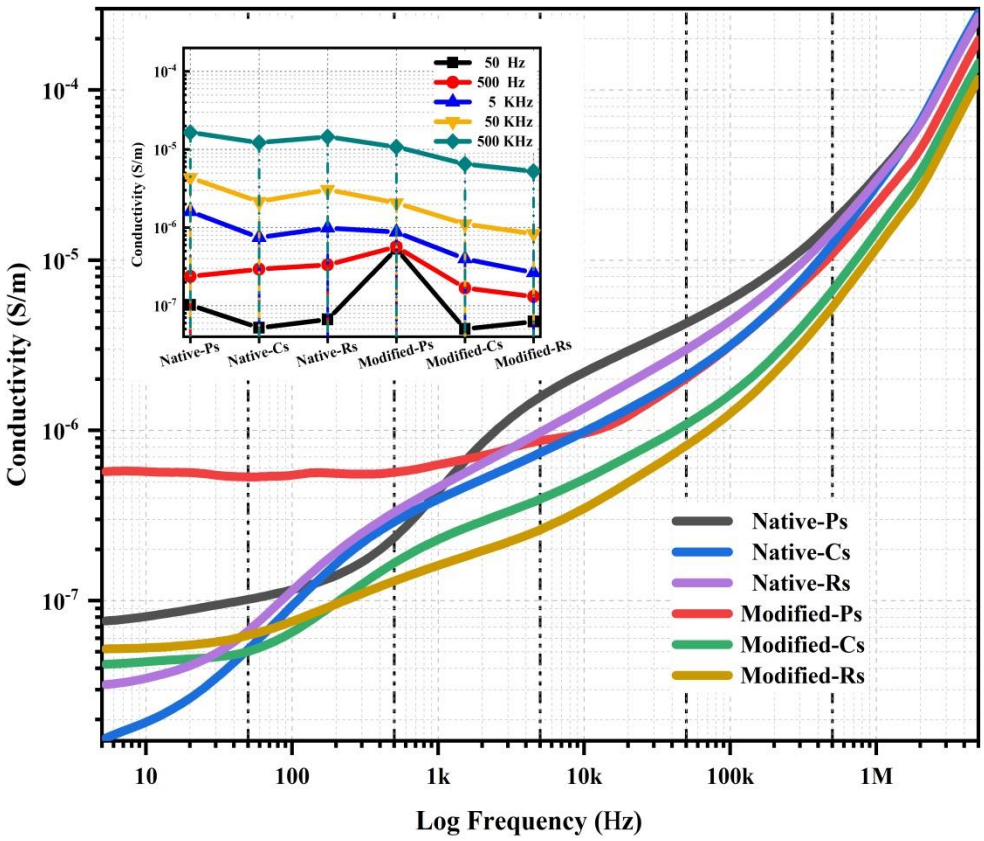

Figure 7. Frequency dependence of σ of native form and modified form of starches over the frequency range of 5 Hz–5 MHz.

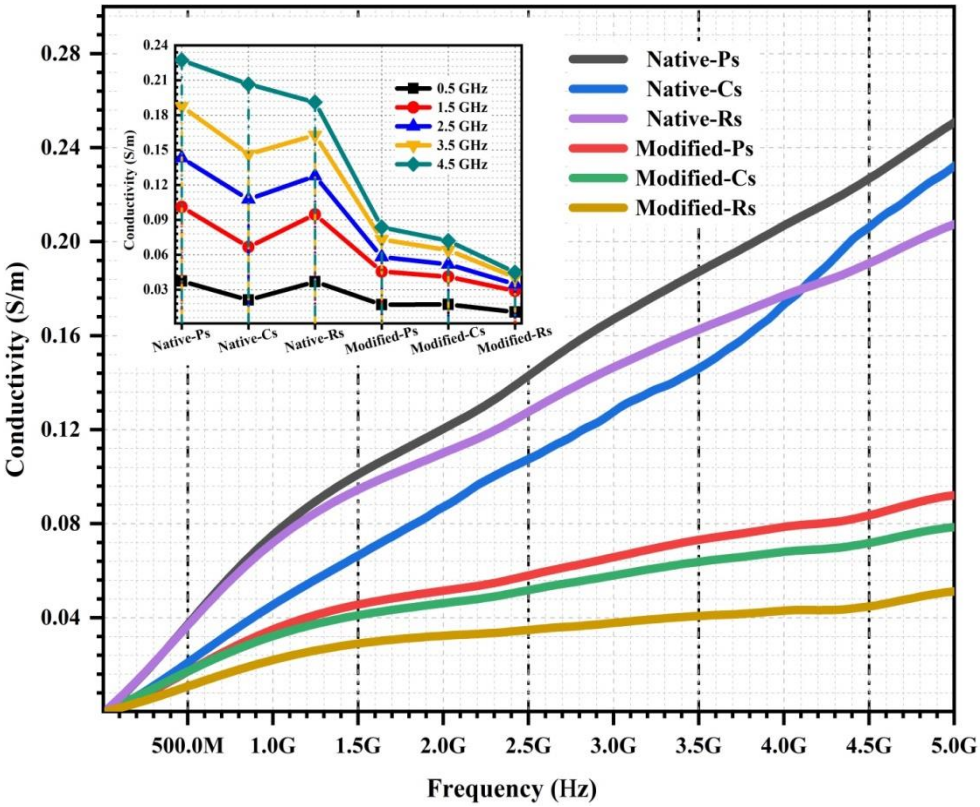

Figure 8. Frequency dependence of σ of native form and modified form of starches over the frequency range of 5 MHz–5 GHz.

At a low frequency (50–500 Hz), the modified-Ps show a more stable σ than the other samples as per the static plateau behavior that can be seen in Figure 7. It can be also shown that the modified-Ps show a higher σ (5.33×10^{-7} S/m) than the modified-Rs (6.26×10^{-8} S/m) and modified-Cs (5.02×10^{-8} S/m) at 50 Hz and 500 Hz. At lower frequencies, the charge carriers get sufficient time to hop, and the mobility of the charge carriers is enhanced by the continuous conductive pathways among the recrystallized potato starches. The larger granular size of the native potato starch is beneficial to the formation of a continuous network structure among starch granule aggregates after hydrothermal modification [8,23,28]. The native-Ps show a higher σ than the other samples, as shown in Figures 7 and 8. A high σ is obviously due to the high amount and mobility of the charge carriers. The native potato starch exhibits a higher σ, which is attributed to the higher number of charge carriers that mainly originate from the polar groups of the amylopectin and phosphorus. On the other hand, the mobility of the charge carriers is enhanced [28,38,39]. The modified starches show a lower σ than the native starches at high frequencies, which may be due to the higher-order continuous network structure and strong hydrogen bonds that restrict the mobility of the charge carriers [28,40]. In addition, the native-Cs (0.21 S/m) exhibit a higher σ than the native-Rs (0.19 S/m) at the frequency of 4.5 GHz, as shown in Figure 8. Different charge carriers in the material system require different amounts of activation energy for the charge carriers to hop from one conductive site to another. The other charge carriers of the native corn starch might be activated with sufficient energy for the charge carrier to hop at a higher frequency range, resulting in a sudden rise in the σ [23,28].

4. Conclusions

The dielectric properties (ε′, ε″, and σ) of starches (potato, corn, and rice starch) in their native and hydrothermally modified forms were investigated in the 5 Hz–5 GHz range. Overall, the dielectric properties of modified starches from 5 Hz–5 GHz are lower than that of native starches. This is due to the disruption of the polysaccharide's molecular

structure in terms of arrangement within the starch granule. The modified potato starch illustrates a higher ε'' and a more stable σ at 50 Hz and 500 Hz than the other starches. This can be attributed to the larger continuous network structure of the potato starch after hydrothermal modification. The modification enhances the energy dissipation during the interfacial polarization. The rice starch exhibits the largest difference in ε' and ε'' between the modified and the native form over the frequency range of 5 MHz–5 GHz. This is attributed to the charge immobilization induced by the formation of abundant intermolecular bonds in the closely packed structure after recrystallization. In the meantime, the relaxation peaks of ε'' can be noticed at 0.5 GHz and 4.5 GHz. The relaxation peaks are mainly attributed to the effect of the hydroxyl side groups and hydroxymethyl side group of the starches, which have strong permanent dipole moments. The results of this work provide a new perspective on material characterization, and the dielectric characterization has a promising potential for quality assessment in starch-based plastic development.

Author Contributions: Conceptualization, E.M.C.; methodology, C.Y.B. and S.F.K.; software, K.Y.L.; validation, E.M.C. and N.F.M.N.; formal analysis, M.S.A.M. and S.F.K.; investigation, C.Y.B. and M.S.A.M.; resources, M.R.M.J.; data curation, E.Z.M.T.; writing—original draft preparation, C.Y.B.; writing—review and editing, E.M.C. and N.F.M.N.; visualization, K.Y.L.; supervision, E.M.C. and N.F.M.N.; project administration, M.R.M.J.; funding acquisition, E.M.C. All authors have read and agreed to the published version of the manuscript.

Funding: This research was funded by the Fundamental Research Grant Scheme (FRGS) from the Ministry of Higher Education Malaysia with grant number: RACER/1/2019/STG07/UNIMAP/2. The APC was funded by Universiti Malaysia Perlis (UniMAP).

Institutional Review Board Statement: Not applicable.

Informed Consent Statement: Not applicable.

Data Availability Statement: Not applicable.

Acknowledgments: All authors would like to express their sincere gratitude to all technical staffs from the Laboratory of Biomaterial at Universiti Malaysia Perlis (UniMAP) for their technical advice and assistance.

Conflicts of Interest: The authors declare no conflict of interest.

References

1. Zhu, Z.; Guo, W. Frequency, moisture content, and temperature dependent dielectric properties of potato starch related to drying with radio-frequency/microwave energy. *Sci. Rep.* **2017**, *7*, 9311. [CrossRef] [PubMed]
2. Drakopoulos, S.X.; Karger-Kocsis, J.; Kmetty, Á.; Lendvai, L.; Psarras, G.C. Thermoplastic starch modified with microfibrillated cellulose and natural rubber latex: A broadband dielectric spectroscopy study. *Carbohydr. Polym.* **2017**, *157*, 711–718. [CrossRef] [PubMed]
3. Meena; Sharma, A. Dielectric spectroscopy of Ag-starch nanocomposite films. *Mater. Res. Express* **2018**, *5*, 045041. [CrossRef]
4. Braşoveanu, M.; Nemţanu, M.R. Behaviour of starch exposed to microwave radiation treatment. *Starch-Stärke* **2014**, *66*, 3–14. [CrossRef]
5. Nafchi, A.M.; Moradpour, M.; Saeidi, M.; Alias, A.K. Thermoplastic starches: Properties, challenges, and prospects. *Starch-Stärke* **2013**, *65*, 61–72. [CrossRef]
6. Marichelvam, M.K.; Jawaid, M.; Asim, M. Corn and rice starch-based bio-plastics as alternative packaging materials. *Fibers* **2019**, *7*, 32. [CrossRef]
7. García, M.A.; Barbosa, S.E.; Castillo, L.A.; Olivia, V.L.; Villar, M.A. Crystalline morphology of thermoplastic starch/talc nanocomposites induced by thermal processing. *Heliyon* **2019**, *5*, e01877. [CrossRef]
8. Bajaj, R.; Singh, N.; Kaur, A.; Inouchi, N. Structural, morphological, functional and digestibility properties of starches from cereals, tubers and legumes: A comparative study. *J. Food Sci. Technol.* **2018**, *55*, 3799–3808. [CrossRef]
9. Tao, Y.; Yan, B.; Fan, D.; Zhang, N.; Ma, S.; Wang, L.; Wu, Y.; Wang, M.; Zhao, J.; Zhang, H.; et al. Structural changes of starch subjected to microwave heating: A review from the perspective of dielectric properties. *Trends Food Sci. Technol.* **2020**, *99*, 593–607. [CrossRef]
10. Mamat, H.; Hill, S.E. Structural and functional properties of major ingredients of biscuit. *Int. Food Res. J.* **2018**, *25*, 462–471.
11. Vamadevan, V.; Bertoft, E. Structure-function relationships of starch components. *Starch-Stärke* **2015**, *67*, 55–68. [CrossRef]

12. Waterschoot, J.; Gomand, S.V.; Fierens, E.; Delcour, J.A. Production, structure, physicochemical and functional properties of maize, cassava, wheat, potato and rice starches. *Starch-Stärke* **2015**, *67*, 14–29. [CrossRef]
13. Ghoshal, S.; Mattea, C.; Denner, P.; Stapf, S. Effect of initial conformation on the starch biopolymer film formation studied by NMR. *Molecules* **2020**, *25*, 1227. [CrossRef] [PubMed]
14. Huang, V.T.; Perdon, A.A. Major changes in cereal biopolymers during ready-to-eat cereal processing. In *Breakfast Cereals and How They Are Made*; Perdon, A.A., Schonauer, S.L., Poutanen, K.S., Eds.; Elsevier Inc.: Amsterdam, The Netherlands, 2020; pp. 109–140. ISBN 9780128120439.
15. Bansal, N.; Dhaliwal, A.S.; Mann, K.S. Dielectric properties of corn flour from 0.2 to 10 GHz. *J. Food Eng.* **2015**, *166*, 255–262. [CrossRef]
16. Wang, S.; Copeland, L. Molecular disassembly of starch granules during gelatinization and its effect on starch digestibility: A review. *Food Funct.* **2013**, *4*, 1564–1580. [CrossRef]
17. Zhang, B.; Dhital, S.; Gidley, M.J. Densely packed matrices as rate determining features in starch hydrolysis. *Trends Food Sci. Technol.* **2015**, *43*, 18–31. [CrossRef]
18. Wang, S.; Li, C.; Copeland, L.; Niu, Q.; Wang, S. Starch retrogradation: A comprehensive review. *Compr. Rev. Food Sci. Food Saf.* **2015**, *14*, 568–585. [CrossRef]
19. Li, M.; Dhital, S.; Wei, Y. Multilevel structure of wheat starch and its relationship to noodle eating qualities. *Compr. Rev. Food Sci. Food Saf.* **2017**, *16*, 1042–1055. [CrossRef]
20. Wang, W.; Zheng, B.; Tian, Y. Functional group changes and chemical bond-dependent dielectric properties of lotus seed flour with microwave vacuum drying. *J. Food Sci.* **2020**, *85*, 4241–4248. [CrossRef]
21. Rayssi, C.; El Kossi, S.; Dhahri, J.; Khirouni, K. Frequency and temperature-dependence of dielectric permittivity and electric modulus studies of the solid solution $Ca_{0.85}Er_{0.1}Ti_{1-x}Co_{4x/3}O_3$ ($0 \leq x \leq 0.1$). *RSC Adv.* **2018**, *8*, 17139–17150. [CrossRef]
22. Abd El-Kader, M.F.H.; Ragab, H.S. DC conductivity and dielectric properties of maize starch/methylcellulose blend films. *Ionics* **2013**, *19*, 361–369. [CrossRef]
23. Bin-Dahman, O.A.; Rahaman, M.; Khastgir, D.; Al-Harthi, M.A. Electrical and dielectric properties of poly (vinyl alcohol)/starch/graphene nanocomposites. *Can. J. Chem. Eng.* **2018**, *96*, 903–911. [CrossRef]
24. Ahmad, Z. Polymeric dielectric materials. In *Dielectric Material*; Silaghi, M.A., Ed.; InTechOpen: London, UK, 2012; pp. 3–26. ISBN 978-953-51-0764-4.
25. Chakraborty, I.; Pallen, S.; Shetty, Y.; Roy, N.; Mazumder, N. Advanced microscopy techniques for revealing molecular structure of starch granules. *Biophys. Rev.* **2020**, *12*, 105–122. [CrossRef] [PubMed]
26. Jiang, H.; Zhang, M.; Fang, Z.; Mujumdar, A.S.; Xu, B. Effect of different dielectric drying methods on the physic-chemical properties of a starch–water model system. *Food Hydrocoll.* **2016**, *52*, 192–200. [CrossRef]
27. Tao, J.; Cao, S.A. Flexible high dielectric thin films based on cellulose nanofibrils and acid oxidized multi-walled carbon nanotubes. *RSC Adv.* **2020**, *10*, 10799–10805. [CrossRef]
28. Mrudula, M.S.; Nair, M.G. Dielectric properties of natural rubber/polyethylene oxide block copolymer complexed with transition metal ions. *Polym. Bull.* **2020**, *77*, 6029–6048. [CrossRef]
29. Sivakumar, D.; Premkumar, S.; Madankumar, M.; Manivannan, M. Structural characterization and dielectric properties of starch coated magnetite nanoparticles. *J. Emerg. Technol. Innov. Res.* **2018**, *5*, 61–72.
30. Cheng, E.M.; You, K.Y.; Lee, K.Y.; Abbas, Z.; Rahim, H.A.; Khor, S.F.; Zakaria, Z.; Lee, Y.S. Dielectric spectroscopy technique for carbohydrate characterization of fragrant rice, brown rice and white rice. In Proceedings of the 2017 Progress in Electromagnetics Research Symposium-Fall (PIERS-FALL), Singapore, 19–22 November 2017; pp. 205–209.
31. Wang, J.; Lim, E.G.; Leach, M.P.; Wang, Z.; Man, K.L. Open-ended coaxial cable selection for measurement of liquid dielectric properties via the reflection method. *Math. Probl. Eng.* **2020**, *2020*, 8942096. [CrossRef]
32. Seth, A.; Shah, B. Morphology of different parts of medicinal plant. In *A Textbook of Pharmacognosy and Phytochemistry*; Chauhan, S.K., Ed.; Elsevier Inc.: New Delhi, India, 2009; pp. 29–56. ISBN 9788131222980.
33. Supriya, S.; Kumar, S.; Kar, M. Grain size and grain boundary effect on dielectric behavior of nanocrystalline cobalt ferrite. In Proceedings of the 2017 IEEE 12th Nanotechnology Materials and Devices Conference (NMDC), Singapore, 2–4 October 2017; pp. 165–166.
34. Kiliç, M.; Karabul, Y.; Özdemir, Z.G.; Erdönmez, S.; Bulgurcuoğlu, A.E.; Yeşilkaya, S.S.; Okutan, M.; İçelli, O. Effect of borax additive on the dielectric response of polypyrrole. *Bull. Mater. Sci.* **2018**, *41*, 52. [CrossRef]
35. Krithika, P.L.; Ratnamala, K. Modification of starch: A review of various techniques. *Int. J. Res. Anal. Rev.* **2019**, *6*, 32–45.
36. Xu, B.; Yi, X.; Huang, T.; Zheng, Z.; Zhang, J.; Salehi, A.; Coropceanu, V.; Hoi, C.; Ho, Y.; Marder, S.R.; et al. Donor conjugated polymers with polar side chain groups: The role of dielectric constant and energetic disorder on photovoltaic performance. *Adv. Funct. Mater.* **2018**, *28*, 1803418. [CrossRef]
37. Ohki, Y.; Tajitsu, Y.; Kohtoh, M.; Okabe, S. Dielectric properties of biodegradable polylactic acid and starch ester. In Proceedings of the 2004 IEEE International Conference on Solid Dielectrics, Toulouse, France, 5–9 July 2004; pp. 87–89.
38. Domene-l, D.; Carlos, J.; Martin-gullon, I.; Montalb, M.G. Influence of starch composition and molecular weight on physicochemical properties of biodegradable films. *Polymers* **2019**, *11*, 1084. [CrossRef] [PubMed]

39. Chatterjee, B.; Kulshrestha, N.; Gupta, P.N. Nano composite solid polymer electrolytes based on biodegradable polymers starch and poly vinyl alcohol. *Measurement* **2016**, *82*, 490–499. [CrossRef]
40. Zyane, A.; Belfkira, A.; Brouillette, F.; Lucas, R.; Marchet, P. Microcrystalline cellulose as a green way for substituting $BaTiO_3$ in dielectric composites and improving their dielectric properties. *Cellul. Chem. Technol.* **2015**, *49*, 783–787.